

Neural Networks Are Implicit Decision Trees: The Hierarchical Simplicity Bias

Zhehang Du*

November 7, 2023

Abstract

Neural networks exhibit simplicity bias; they rely on simpler features while ignoring equally predictive but more complex features. In this work, we introduce a novel approach termed *imbalanced label coupling* to investigate scenarios where simple and complex features exhibit different levels of predictive power. In these cases, complex features still contribute to predictions. The trained networks make predictions in alignment with the ascending complexity of input features according to how they correlate with the label in the training set, irrespective of the underlying predictive power. For instance, even when simple spurious features distort predictions in CIFAR-10, most cats are predicted to be dogs, and most trucks are predicted to be automobiles! This observation provides direct evidence that the neural network learns core features in the presence of spurious features. We empirically show that last-layer retraining with target data distribution [Kirichenko et al., 2022] is effective, yet insufficient to fully recover core features when spurious features are perfectly correlated with the target labels in our synthetic dataset. We hope our research contributes to a deeper understanding of the implicit bias of neural networks.

1 Introduction

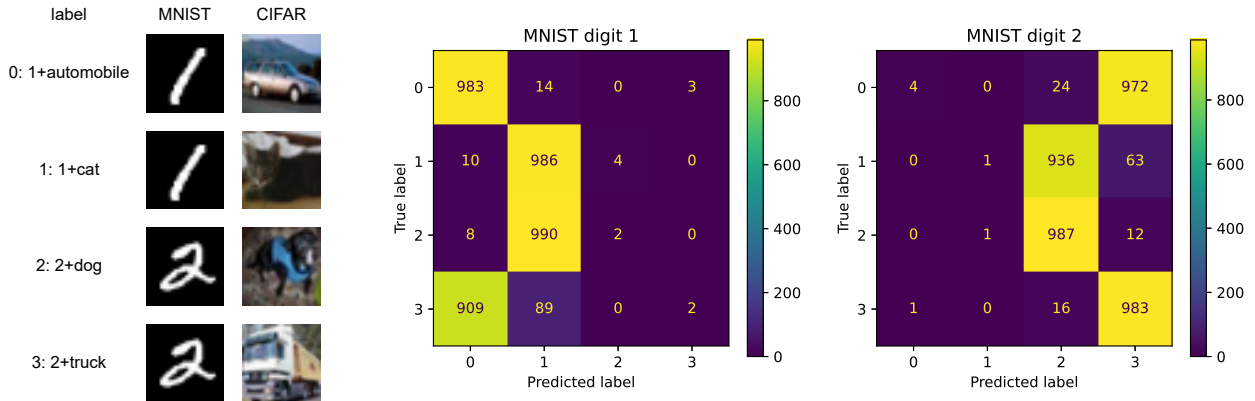
In machine learning, neural networks (NNs) have shown remarkable abilities to learn and generalize from data even with over-parametrization, known as double descent [Nakkiran et al., 2021]. Despite their adeptness, neural networks can exhibit vulnerability when faced with real-world challenges like distribution shifts [Hendrycks et al., 2021] and adversarial attacks [Szegedy et al., 2013, Madry et al., 2017]. The simplicity bias [Valle-Perez et al., 2018, Kalimeris et al., 2019, Shah et al., 2020, Pezeshki et al., 2021] has been proposed that aims to address the underlying mechanism. It is the propensity of gradient descent that is biased toward learning simple and strongly correlated features than more complex but robust features. This preference for simplicity might seem reasonable, as this inductive bias naturally reflects the properties of real-world data and leads to generalization [Teney et al., 2022]. However, it can lead to models that struggle when subjected to distributional shifts and adversarial attacks.

Neural networks also show vulnerability to spurious features that introduce false associations with the target labels and are ubiquitous in real-world applications, degrading model performance [Sagawa et al., 2019]. A large body of work has been developed to mitigate the vulnerability of

*Independent researcher; Email: dzhehang@mail.ustc.edu.cn.

neural networks to spurious correlations, making it vital to study how core features are learned in the presence of spurious features [Izmailov et al., 2022]. To contribute to this line of work, in this study, we present an interesting finding that directly evidences the neural network’s ability to utilize the core features in the presence of spurious features. By examining the confusion matrix of the trained network on our synthetic dataset, we reveal an interesting hierarchical decision-making behavior that is inherently related to the complexity of the features.

Proposed method. We use a novel approach called *imbalanced label coupling* to create the training set. The MNIST-CIFAR dataset is presented in Figure 1a. The dataset contains images that concatenate MNIST digits and CIFAR-10 images channel-wise. Contrary to the extreme simplicity bias where a single MNIST digit matches one CIFAR-10 class [Shah et al., 2020], we concatenate one type of MNIST digit with multiple CIFAR-10 classes, with the label determined by the CIFAR-10 image. In this context, MNIST digits serve as spurious correlations, while CIFAR-10 images represent core features. The objective is to evaluate the model’s ability to correctly classify CIFAR-10 images when paired with different MNIST digits. For testing, we remove the coupling constraints, concatenating each MNIST digit with each CIFAR-10 class.



(a) The training set.

(b) The confusion matrices on the test set with two types of MNIST digits.

Figure 1: The MNIST-CIFAR training set and test results. **(a)** Within the training set, digit 1 is concatenated with both automobile and cat images, while digit 2 is concatenated with both dog and truck images. **(b)** During testing, most digit 1 samples are classified 0 and 1, while most digit 2 samples are classified 2 and 3, regardless of the corresponding CIFAR-10 image class.

As shown in Figure 1b, the MNIST channel dominantly influences the classification results. Interestingly, misclassifications are not randomly distributed among incorrect classes when CIFAR-10 images are coupled with different MNIST digits during training. The CIFAR-10 channels retain some predictive power; for instance, most automobile images are misclassified as trucks, and cats as dogs, reflecting the inherent similarities in true object semantics. The behavior of the trained neural network resembles that of a decision tree, as illustrated in Figure 2.

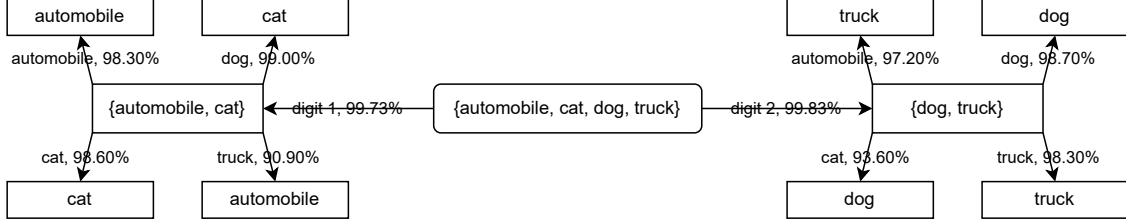


Figure 2: The inferred decision tree from the neural network trained on the MNIST-CIFAR dataset. Enclosed within the box are the neural network’s predictions, while the arrow text denotes the ground truth image. The percentage indicates the proportion of sample predictions aligned with the classes listed in the box. To illustrate, among all MNIST digit 1 images, approximately 99.73% are categorized within classes {automobile, cat}. Furthermore, 99.00% of images concatenating both a dog and digit 1 fall under the cat class.

Organization. In Section 2, we discuss the related work. Section 3 outlines the construction of synthesized datasets, designed to elicit decision-tree-like behavior from the trained neural networks, extending up to three levels. Additionally, we discuss the implications of applying the Deep Feature Reweighting method [Kirichenko et al., 2022] to our synthetic dataset. In Section 4, we demonstrate that this decision-tree-like behavior persists across varying background colors (Subsection 4.1) and several image distortions (Subsection 4.2).

2 Related Work

Simplicity bias. Simplicity bias is the tendency of neural networks to learn simple functions, potentially leading to suboptimal generalization and vulnerability to adversarial attacks [Shah et al., 2020]. Kalimeris et al. [2019] show that stochastic gradient descent learns functions of increasing complexity. Soudry et al. [2018], Gunasekar et al. [2018], Nacson et al. [2019], Lyu et al. [2021], Kunin et al. [2022] show that gradient descent leads to max-margin classifiers. Gunasekar et al. [2017], Arora et al. [2019], Huh et al. [2021] show that deep networks are inductively biased to find low-rank solutions. Valle-Perez et al. [2018] show that the parameter-function map is biased towards simple functions with algorithmic information theory. Pezeshki et al. [2021] propose gradient starvation. Morwani et al. [2023] rigorously study simplicity bias in one hidden layer neural networks. Cao et al. [2019], Rahaman et al. [2019] study the spectral bias of deep neural networks.

As shown by Shah et al. [2020], models can exhibit extreme simplicity bias, relying solely on simpler features while ignoring equally or more predictive complex ones. For example, in their MNIST-CIFAR dataset, images in class -1 are concatenations of MNIST digit zero and CIFAR-10 automobiles, while images in class 1 are concatenations of MNIST digit one and CIFAR-10 trucks. The trained network only depends on the MNIST digit for classification. Another example is found in shortcut learning [Geirhos et al., 2020], where the neural network focuses on object location rather than object type. Taking a step further, our study reveals a more nuanced perspective. Complex features are not entirely ignored but can retain their predictive power. Our findings do not contradict prior research where simple features have complete predictive power. Rather, in our experiments, simple features serve as predictive indicators only for the specific subgroups trained with those features. Thus, our work extends earlier research: where extreme simplicity bias is similar to a single-level decision tree, our approach resembles a multi-level decision tree.

Spurious correlations. Neural networks exhibit bias towards spurious features, which are only associated with the task label but are not causally related [Geirhos et al., 2020]. Such biases have been found in real-world image datasets [Singla and Feizi, 2021, Singla et al., 2021]. Such features include texture [Geirhos et al., 2018], poses [Alcorn et al., 2019], and background [Geirhos et al., 2018, Moayeri et al., 2022]. Overparametrization’s negative impact on model performance in the context of these spurious correlations is investigated by Sagawa et al. [2020]. Further, studies have been conducted to understand the influencing factors of feature representations [Hermann and Lampinen, 2020] and to identify likely shortcut cues [Scimeca et al., 2021]. Mitigation methods include distributionally robust optimization (DRO) targeting worst-group loss instead of average loss [Ben-Tal et al., 2013, Hu et al., 2018, Sagawa et al., 2019, Zhang et al., 2020], invariant learning [Arjovsky et al., 2019, Koyama and Yamaguchi, 2020, Creager et al., 2021, Yao et al., 2022], and weighting [Nam et al., 2020, Liu et al., 2021, Zhang et al., 2022].

In closely related works, Kirichenko et al. [2022], Rosenfeld et al. [2022] demonstrate that despite spurious correlations, neural networks capture core features that can be recovered by retraining the final layer with target distribution data. Our work, on the other hand, investigates the confusion matrix, highlighting the network’s inherent reliance on true object semantics in the presence of spurious features, without training a feature representation decoder. We also show that last-layer retraining is insufficient to fully capture the network’s ability to utilize core features. Similarly, Ye et al. [2023] provide a theoretical analysis of last-layer retraining for two-layer networks, proving that core features are only learned well when their associated non-realizable noise is small.

3 Hierarchical Simplicity Bias and Feature Complexity

3.1 Experiment Setup

Building blocks. (1) Patch: Our dataset includes four types of patch data, each sized at 32×32 and 1 channel. These patches feature a white corner with the remaining area in black, as in Figure 3. The patch data is deterministic. (2) MNIST [LeCun et al., 2010]: the MNIST dataset’s images are subjected to zero padding, extending them from their original dimensions of 28×28 to 32×32 . (3) CIFAR-10 [Krizhevsky et al., 2009].

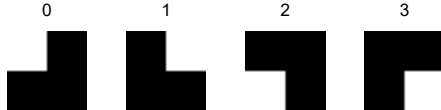


Figure 3: The patch data types. Type 0, 1, 2, and 3 have a white patch in the upper-left, upper-right, lower-left, and lower-right corners respectively.

Training set. The training set is created through *imbalanced label coupling*. We choose two different datasets: one with coarse labels and another with fine labels. For each class from the coarse dataset, we concatenate it with multiple classes from the fine dataset to create the training examples. We assign labels to these examples based on the fine dataset. In other words, the fine dataset has full predictive power, while the coarse dataset does not. Across all experiments, every class comprises 5000 training examples, and the total number of classes is the number of classes chosen in the fine dataset. This construction can be naturally extended to three or more datasets.

For instance, we form the MNIST-CIFAR dataset by concatenating the CIFAR-10 image with dimensions $3 \times 32 \times 32$ and the expanded MNIST digit with dimensions $1 \times 32 \times 32$ to generate a new image with dimensions $4 \times 32 \times 32$.

Test set. The test set is created by concatenating the image channels from all selected classes in each dataset, without any coupling constraints. Each potential combination results in 1000 test samples. Hence, the overall test sample count equals 1000 multiplied by the product of the selected class counts in each dataset.

Network architecture and training configuration. We use the ResNet-18 architecture [He et al., 2016], only making slight adjustments to align the channel of the initial convolutional filter with the input and output dimensions to match the class count. We train the model for 150 epochs using the SGD optimizer with a momentum of 0.9, employing a batch size of 128. The initial learning rate is 0.1, and is reduced by a factor of 10 at epochs 50 and 100. We apply a weight decay of 0.0005. The loss function used for training is the cross-entropy loss. For more experiments on the multilayer perceptron (MLP), see Appendix A.

3.2 Experiment results

MNIST-CIFAR hierarchy. We use MNIST as the coarse data and CIFAR-10 as the fine data in the MNIST-CIFAR training set, shown in Figure 1. Conversely, the CIFAR-MNIST training set is shown in Figure 4. The neural network consistently gives priority to MNIST regardless of its predictive power. The CIFAR-10 part only comes into play when MNIST’s predictive power is insufficient. Hence, MNIST exhibits a strictly simpler complexity than CIFAR-10.

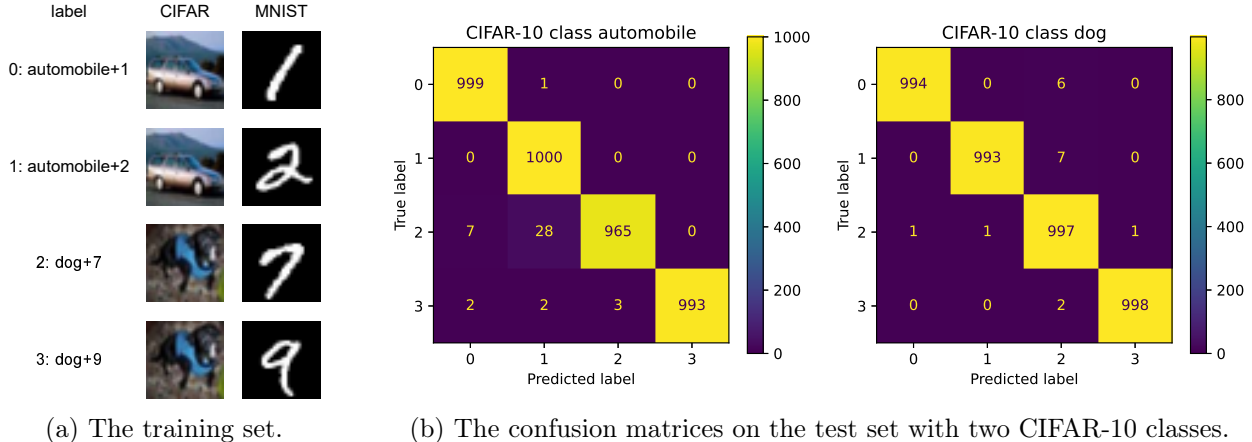


Figure 4: The CIFAR-MNIST training set and test results. **(a)** The training set includes automobile images paired with 1 and 2 digits, along with cat images paired with 7 and 9 digits. **(b)** During testing, predictions rely mostly on MNIST and exhibit high accuracy.

Patch-MNIST Hierarchy. Similarly, we construct the training set of Patch-MNIST and MNIST-Patch. Figure 5 and Figure 6 show the training set and test results. These results highlight the hierarchy that patch data is inherently less complex than MNIST. Interestingly, predictions are not

completely random with spurious patch data in Figure 5. For instance, when comparing digits 1 and 2, digit 2 has the closest visual similarity to digits 7 and 9 (and vice versa for digit 7). As a result, a large portion of digits 7 and 9 are categorized under digit 2 rather than digit 1.

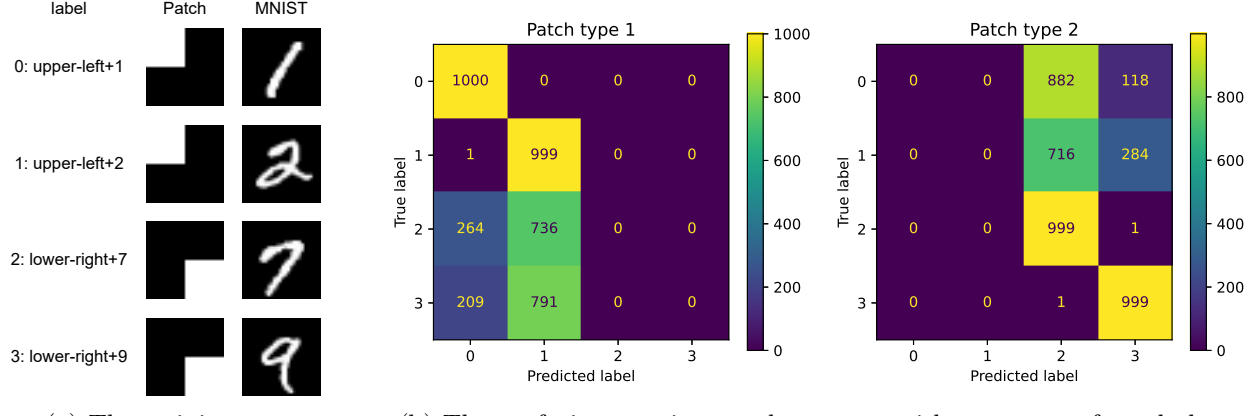


Figure 5: The Patch-MNIST training set and test results. **(a)** The upper-left patch is paired with 1 and 2 digits, along with the lower-right patch paired with 7 and 9 digits. **(b)** In testing, all predictions prioritize patch data without any exceptions.

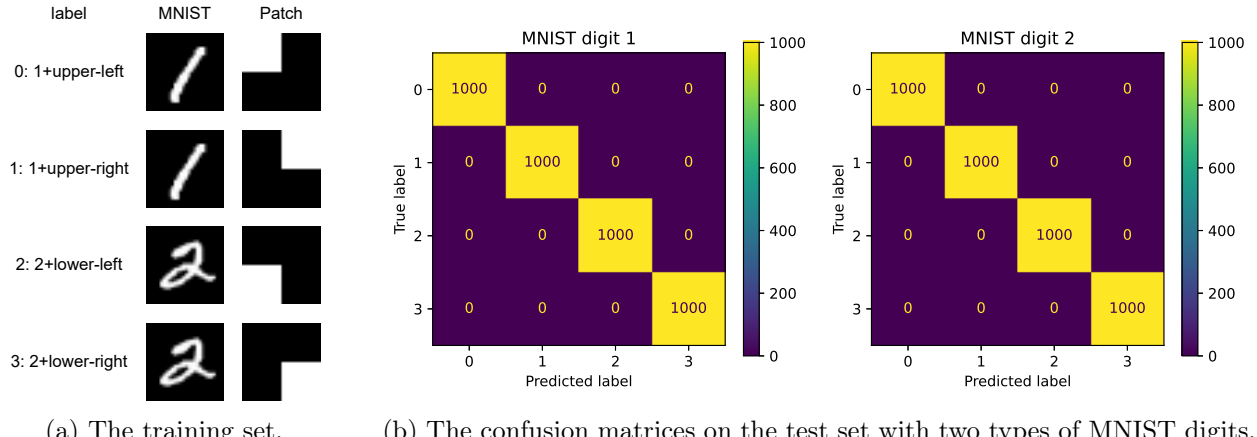


Figure 6: The MNIST-Patch training set and test results. **(a)** Digit 1 is paired with upper-left and upper-right patches, and digit 2 is paired with lower-left and lower-right patches. **(b)** The test accuracy achieves 100% using solely patch data.

Patch-MNIST-CIFAR hierarchy. We construct a dataset named Patch-MNIST-CIFAR, containing all aforementioned building blocks, revealing a three-level hierarchy. The upper-left patch is coupled with digits 1 and 2, while the lower-right patch is coupled with digits 5 and 9. These digits (1, 2, 5, 9) are then coupled with CIFAR-10 classes (0, 1), (2, 3), (4, 5), and (6, 7) respectively, resulting in an 8-class dataset. The results are shown in Figure 7. The neural network demonstrates a distinct hierarchy in its predictions based on increasing feature complexity: first patch data, then MNIST digits, and finally CIFAR-10 images.

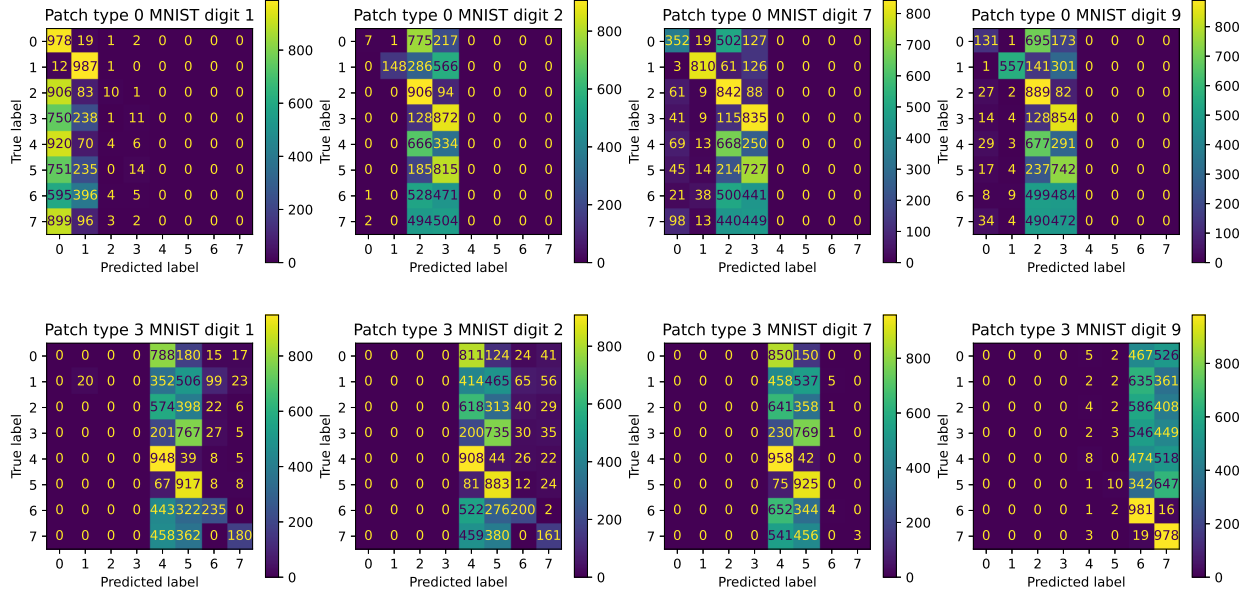


Figure 7: The confusion matrices of the network trained on the Patch-MNIST-CIFAR dataset.

3.3 Discussion on Deep Feature Reweighting

Kirichenko et al. [2022] introduced Deep Feature Reweighting (DFR) to improve model robustness against spurious correlations and distribution shifts by retraining the last layer with test distribution data. We apply DFR to our MNIST-CIFAR dataset, discarding the classification head of the trained model (Figure 1) and retraining it from random initialization with CIFAR and MNIST image concatenations without coupling constraints. The results are presented in Figure 8a. DFR improves the standard accuracy from 49.24% to 68.12%, showing effectiveness in mitigating the effects of spurious correlations to a certain degree. Yet, it falls short of the baseline accuracy of 87.75%, indicating that DFR alone may not completely overcome the challenges posed by spurious features when they are perfectly correlated with the target labels. This observation aligns with Kirichenko et al. [2022], where the worst-group accuracy is only 62% on CIFAR-10 when the spurious correlation level is 100%. The limitation in the final-layer representations’ ability to fully capture and utilize core features implies that some core feature information may be lost in the intermediate layers of the network.

However, confusion matrices show the neural network accurately utilizing core features. In the MNIST-CIFAR dataset, classes 0 and 3 represent vehicles (automobile and truck), while classes 1 and 2 denote animals (dog and cat). We define a semantically correct prediction as one where a vehicle is correctly classified as a vehicle, or an animal is correctly classified as an animal. In Figure 8b, we report both standard accuracy and semantic accuracy. Interestingly, the spurious features do not override the core features associated with these broader categories: the model is capable of identifying broader categorical distinctions (distinguishing between vehicles and animals) even when finer-grained class distinctions are affected. This could be seen as a form of robustness at a higher, more abstract level of understanding. The large gap between standard and semantic accuracies suggests that a deeper understanding of neural network behavior requires looking beyond just overall accuracy and considering how models perform across different levels of abstraction.

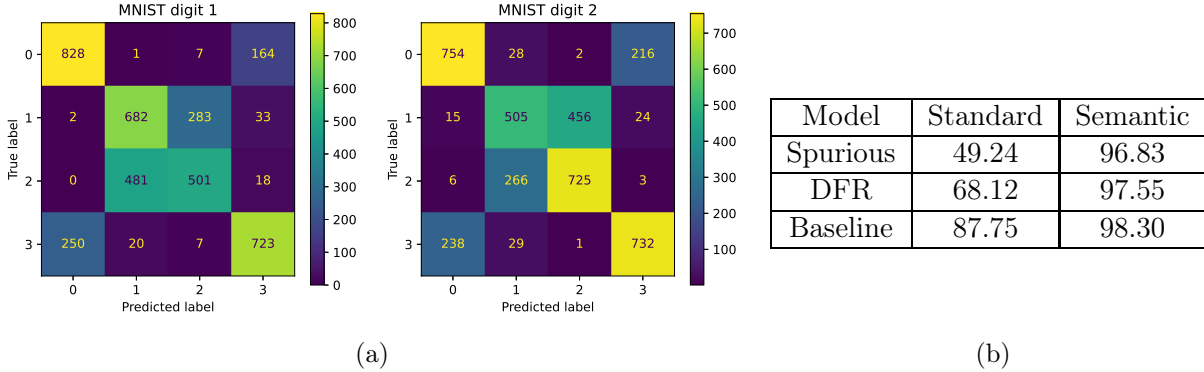


Figure 8: (a) Confusion matrices following DFR of the neural network trained on the MNIST-CIFAR dataset in Figure 1. (b) Performance comparison of three models: Spurious (trained on the MNIST-CIFAR dataset), DFR (the Spurious model after DFR), and Baseline (trained on CIFAR-10 images), measured in both standard accuracy (%) and semantic accuracy (%).

4 Background and Corruption Hierarchy

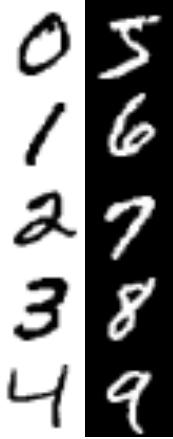
It has been demonstrated that neural networks exhibit a bias for texture and background [Geirhos et al., 2018, Moayeri et al., 2022]. In this section, we present similar evidence of decision-tree-like behavior in scenarios involving different background colors and image corruptions. The network architecture and training setups are the same as those in Section 3.

4.1 Background Hierarchy in Half-Inverted MNIST

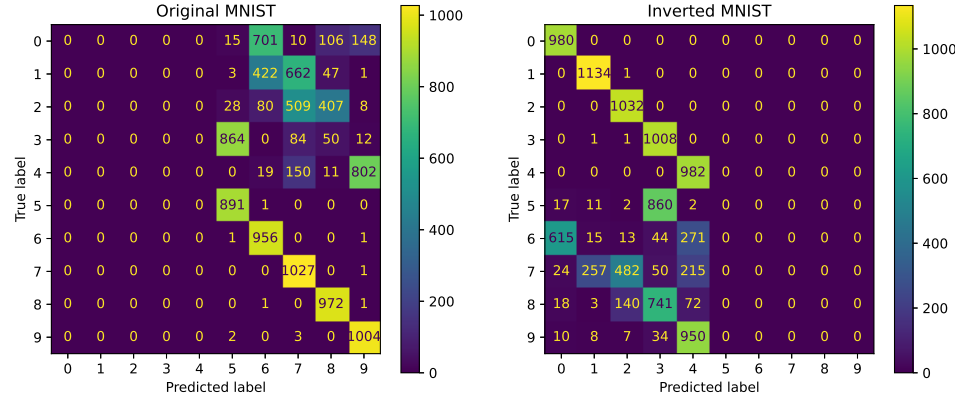
During training, we inverted the colors of MNIST digits 0-4 while leaving digits 5-9 unchanged. We tested the model using both the original and color-inverted test sets, with the results shown in Figure 9. The neural network consistently categorized white-background samples as 0-4 and black-background samples as 5-9, even though MNIST digits are nearly linearly separable. Unlike the ColorMNIST dataset in Zhang et al. [2022] that uses five different background colors, our study uses just two (and also inverts the color of the digits themselves), which helps to better visualize the hierarchical decision-making process: most occurrences of digit 4 are wrongly classified as 9, and most of digit 3 as 5, and vice versa.

4.2 Corruption Hierarchy in Corrupted CIFAR-10

We subject the CIFAR-10 training set to four common types of corruptions [Hendrycks and Dietterich, 2019]: Gaussian noise, Defocus blur, Fog, and Brightness, all with a severity level of 3. For detailed implementations, see Hendrycks and Dietterich [2019]. Each type of corruption is applied to specific CIFAR-10 classes: (0, 1), (2, 3), (4, 5), and (6, 7), while classes (8, 9) remain uncorrupted. The test set includes the original test set with 10,000 samples, as well as the four corrupted versions of the test set, yielding a combined dataset of 50,000 samples. The results are in Figure 10. The hierarchical behavior is not easily visualizable under this setting as there are a total of five groups subjected to different corruptions. Nevertheless, the classification results are not uniformly randomly distributed within each group, which may provide evidence of the hierarchical classification process.



(a) The training set.



(b) The confusion matrices on the original and color-inverted test set.

Figure 9: The half-inverted MNIST dataset and test results. (a) Color inversion applied to digits 0-4; digits 5-9 remain unchanged. (b) During testing, the neural network demonstrates a consistent preference for spurious background colors, with digits of similar shapes exhibiting mutual misclassification.

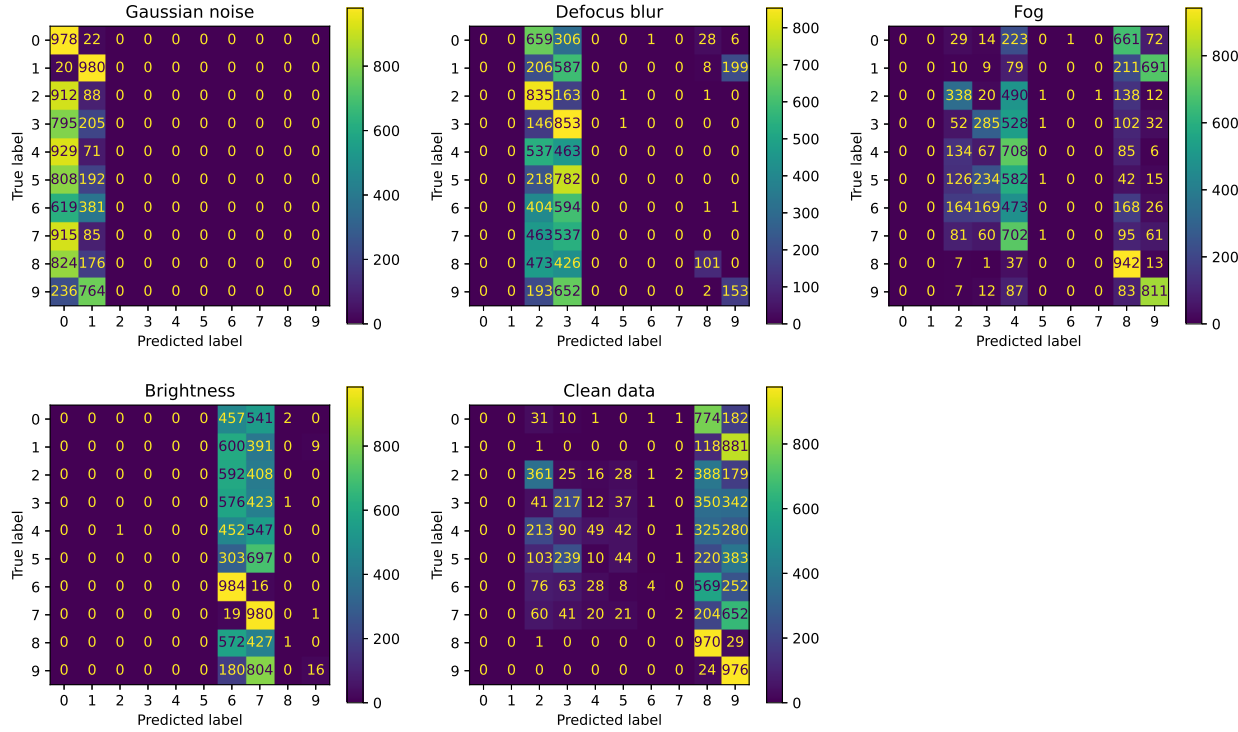


Figure 10: Test results from the neural network trained on the corrupted CIFAR-10 dataset demonstrate that most corruptions heavily influence classification, often leading to predictions falling within the two classes on which they were trained.

5 Conclusion and Future Work

Conclusion. In conclusion, this study explores how core features are learned in the presence of spurious features. We demonstrate that neural networks trained on our synthetic datasets exhibit behavior similar to decision trees. They make predictions that align with the ascending complexity of features, depending on how these features correlate with the labels in the training set, regardless of the underlying predictive power. This hierarchical decision-making pattern emerges when the training set comprises features with varying complexity, when the datasets have different background colors, or when specific types of corruptions are selectively applied to certain classes within the training set. Neural networks still accurately capture some of the semantic information that cannot be fully captured using the last-layer representations when spurious correlations are perfectly associated with the target labels. Our study offers insights into how neural networks prioritize features of varying complexities for prediction, and suggests they might predict through several implicit stages. We hope that our study contributes to a deeper understanding of implicit bias in neural networks and helps in the development of more robust and reliable machine learning systems.

Limitations and future work. In practice, the extreme hierarchical relationships in classifications observed in our study may not be easily observable, as our research is mainly based on synthetic datasets designed to highlight certain behaviors in a controlled setting. Future research could extend these findings to real-world situations, establish a theoretical framework for hierarchical simplicity bias, and propose strategies to mitigate any adverse effects of this bias.

One possible interesting application of our method is to study the similarity between different classes in a dataset. For instance, to examine whether the cat class is more similar to the dog class or the truck class, we can construct the training set by adding one type of simple feature to the cat class images, and adding another type of simple feature to the dog and truck class images. During testing, we change the simple feature in the cat images, and evaluate how likely the cat images will be predicted to be a dog or a truck. The testing result can serve as a measure of how similar these classes are. Another analogous measure is through local elasticity [He and Su, 2019], which considers how the gradient update at one sample impacts the output of another sample.

Acknowledgments

Special thanks to Zhilei Shu for valuable discussions and to Qingyu Hu for reviewing the manuscript. ChatGPT was used for identifying grammatical errors, refining sentences, and aiding in the layout of figures within the LaTeX code.

References

- Michael A Alcorn, Qi Li, Zhitao Gong, Chengfei Wang, Long Mai, Wei-Shinn Ku, and Anh Nguyen. Strike (with) a pose: Neural networks are easily fooled by strange poses of familiar objects. In *Proceedings of the IEEE/CVF conference on computer vision and pattern recognition*, pages 4845–4854, 2019.
- Martin Arjovsky, Léon Bottou, Ishaan Gulrajani, and David Lopez-Paz. Invariant risk minimization. *arXiv preprint arXiv:1907.02893*, 2019.

- Sanjeev Arora, Nadav Cohen, Wei Hu, and Yuping Luo. Implicit regularization in deep matrix factorization. *Advances in Neural Information Processing Systems*, 32, 2019.
- Aharon Ben-Tal, Dick Den Hertog, Anja De Waegenaere, Bertrand Melenberg, and Gijs Rennen. Robust solutions of optimization problems affected by uncertain probabilities. *Management Science*, 59(2):341–357, 2013.
- Yuan Cao, Zhiying Fang, Yue Wu, Ding-Xuan Zhou, and Quanquan Gu. Towards understanding the spectral bias of deep learning. *arXiv preprint arXiv:1912.01198*, 2019.
- Elliot Creager, Jörn-Henrik Jacobsen, and Richard Zemel. Environment inference for invariant learning. In *International Conference on Machine Learning*, pages 2189–2200. PMLR, 2021.
- Robert Geirhos, Patricia Rubisch, Claudio Michaelis, Matthias Bethge, Felix A Wichmann, and Wieland Brendel. Imagenet-trained cnns are biased towards texture; increasing shape bias improves accuracy and robustness. *arXiv preprint arXiv:1811.12231*, 2018.
- Robert Geirhos, Jörn-Henrik Jacobsen, Claudio Michaelis, Richard Zemel, Wieland Brendel, Matthias Bethge, and Felix A Wichmann. Shortcut learning in deep neural networks. *Nature Machine Intelligence*, 2(11):665–673, 2020.
- Suriya Gunasekar, Blake E Woodworth, Srinadh Bhojanapalli, Behnam Neyshabur, and Nati Srebro. Implicit regularization in matrix factorization. *Advances in neural information processing systems*, 30, 2017.
- Suriya Gunasekar, Jason D Lee, Daniel Soudry, and Nati Srebro. Implicit bias of gradient descent on linear convolutional networks. *Advances in neural information processing systems*, 31, 2018.
- Hangfeng He and Weijie J Su. The local elasticity of neural networks. *arXiv preprint arXiv:1910.06943*, 2019.
- Kaiming He, Xiangyu Zhang, Shaoqing Ren, and Jian Sun. Deep residual learning for image recognition. In *Proceedings of the IEEE conference on computer vision and pattern recognition*, pages 770–778, 2016.
- Dan Hendrycks and Thomas Dietterich. Benchmarking neural network robustness to common corruptions and perturbations. *arXiv preprint arXiv:1903.12261*, 2019.
- Dan Hendrycks, Steven Basart, Norman Mu, Saurav Kadavath, Frank Wang, Evan Dorundo, Rahul Desai, Tyler Zhu, Samyak Parajuli, Mike Guo, et al. The many faces of robustness: A critical analysis of out-of-distribution generalization. In *Proceedings of the IEEE/CVF International Conference on Computer Vision*, pages 8340–8349, 2021.
- Katherine Hermann and Andrew Lampinen. What shapes feature representations? exploring datasets, architectures, and training. *Advances in Neural Information Processing Systems*, 33: 9995–10006, 2020.
- Weihua Hu, Gang Niu, Issei Sato, and Masashi Sugiyama. Does distributionally robust supervised learning give robust classifiers? In *International Conference on Machine Learning*, pages 2029–2037. PMLR, 2018.

Minyoung Huh, Hossein Mobahi, Richard Zhang, Brian Cheung, Pulkit Agrawal, and Phillip Isola. The low-rank simplicity bias in deep networks. *arXiv preprint arXiv:2103.10427*, 2021.

Pavel Izmailov, Polina Kirichenko, Nate Gruver, and Andrew G Wilson. On feature learning in the presence of spurious correlations. *Advances in Neural Information Processing Systems*, 35: 38516–38532, 2022.

Dimitris Kalimeris, Gal Kaplun, Preetum Nakkiran, Benjamin Edelman, Tristan Yang, Boaz Barak, and Haofeng Zhang. Sgd on neural networks learns functions of increasing complexity. *Advances in neural information processing systems*, 32, 2019.

Polina Kirichenko, Pavel Izmailov, and Andrew Gordon Wilson. Last layer re-training is sufficient for robustness to spurious correlations. *arXiv preprint arXiv:2204.02937*, 2022.

Masanori Koyama and Shoichiro Yamaguchi. Out-of-distribution generalization with maximal invariant predictor. 2020.

Alex Krizhevsky, Geoffrey Hinton, et al. Learning multiple layers of features from tiny images. 2009.

Daniel Kunin, Atsushi Yamamura, Chao Ma, and Surya Ganguli. The asymmetric maximum margin bias of quasi-homogeneous neural networks. *arXiv preprint arXiv:2210.03820*, 2022.

Yann LeCun, Corinna Cortes, and CJ Burges. Mnist handwritten digit database. *ATT Labs [Online]*, 2, 2010. URL <http://yann.lecun.com/exdb/mnist>.

Evan Z Liu, Behzad Haghgoo, Annie S Chen, Aditi Raghunathan, Pang Wei Koh, Shiori Sagawa, Percy Liang, and Chelsea Finn. Just train twice: Improving group robustness without training group information. In *International Conference on Machine Learning*, pages 6781–6792. PMLR, 2021.

Kaifeng Lyu, Zhiyuan Li, Runzhe Wang, and Sanjeev Arora. Gradient descent on two-layer nets: Margin maximization and simplicity bias. *Advances in Neural Information Processing Systems*, 34:12978–12991, 2021.

Aleksander Madry, Aleksandar Makelov, Ludwig Schmidt, Dimitris Tsipras, and Adrian Vladu. Towards deep learning models resistant to adversarial attacks. *arXiv preprint arXiv:1706.06083*, 2017.

Mazda Moayeri, Phillip Pope, Yogesh Balaji, and Soheil Feizi. A comprehensive study of image classification model sensitivity to foregrounds, backgrounds, and visual attributes. In *Proceedings of the IEEE/CVF Conference on Computer Vision and Pattern Recognition*, pages 19087–19097, 2022.

Depen Morwani, Jatin Batra, Prateek Jain, and Praneeth Netrapalli. Simplicity bias in 1-hidden layer neural networks. *arXiv preprint arXiv:2302.00457*, 2023.

Mor Shpigel Nacson, Jason Lee, Suriya Gunasekar, Pedro Henrique Pamplona Savarese, Nathan Srebro, and Daniel Soudry. Convergence of gradient descent on separable data. In *The 22nd International Conference on Artificial Intelligence and Statistics*, pages 3420–3428. PMLR, 2019.

- Preetum Nakkiran, Gal Kaplun, Yamini Bansal, Tristan Yang, Boaz Barak, and Ilya Sutskever. Deep double descent: Where bigger models and more data hurt. *Journal of Statistical Mechanics: Theory and Experiment*, 2021(12):124003, 2021.
- Junhyun Nam, Hyuntak Cha, Sungsoo Ahn, Jaeho Lee, and Jinwoo Shin. Learning from failure: De-biasing classifier from biased classifier. *Advances in Neural Information Processing Systems*, 33:20673–20684, 2020.
- Mohammad Pezeshki, Oumar Kaba, Yoshua Bengio, Aaron C Courville, Doina Precup, and Guillaume Lajoie. Gradient starvation: A learning proclivity in neural networks. *Advances in Neural Information Processing Systems*, 34:1256–1272, 2021.
- Nasim Rahaman, Aristide Baratin, Devansh Arpit, Felix Draxler, Min Lin, Fred Hamprecht, Yoshua Bengio, and Aaron Courville. On the spectral bias of neural networks. In *International Conference on Machine Learning*, pages 5301–5310. PMLR, 2019.
- Elan Rosenfeld, Pradeep Ravikumar, and Andrej Risteski. Domain-adjusted regression or: Erm may already learn features sufficient for out-of-distribution generalization. *arXiv preprint arXiv:2202.06856*, 2022.
- Shiori Sagawa, Pang Wei Koh, Tatsunori B Hashimoto, and Percy Liang. Distributionally robust neural networks for group shifts: On the importance of regularization for worst-case generalization. *arXiv preprint arXiv:1911.08731*, 2019.
- Shiori Sagawa, Aditi Raghunathan, Pang Wei Koh, and Percy Liang. An investigation of why overparameterization exacerbates spurious correlations. In *International Conference on Machine Learning*, pages 8346–8356. PMLR, 2020.
- Luca Scimeca, Seong Joon Oh, Sanghyuk Chun, Michael Poli, and Sangdoo Yun. Which short-cut cues will dnns choose? a study from the parameter-space perspective. *arXiv preprint arXiv:2110.03095*, 2021.
- Harshay Shah, Kaustav Tamuly, Aditi Raghunathan, Prateek Jain, and Praneeth Netrapalli. The pitfalls of simplicity bias in neural networks. *Advances in Neural Information Processing Systems*, 33:9573–9585, 2020.
- Sahil Singla and Soheil Feizi. Salient imagenet: How to discover spurious features in deep learning? *arXiv preprint arXiv:2110.04301*, 2021.
- Sahil Singla, Besmira Nushi, Shital Shah, Ece Kamar, and Eric Horvitz. Understanding failures of deep networks via robust feature extraction. In *Proceedings of the IEEE/CVF Conference on Computer Vision and Pattern Recognition*, pages 12853–12862, 2021.
- Daniel Soudry, Elad Hoffer, Mor Shpigel Nacson, Suriya Gunasekar, and Nathan Srebro. The implicit bias of gradient descent on separable data. *The Journal of Machine Learning Research*, 19(1):2822–2878, 2018.
- Christian Szegedy, Wojciech Zaremba, Ilya Sutskever, Joan Bruna, Dumitru Erhan, Ian Goodfellow, and Rob Fergus. Intriguing properties of neural networks. *arXiv preprint arXiv:1312.6199*, 2013.

Damien Teney, Ehsan Abbasnejad, Simon Lucey, and Anton Van den Hengel. Evading the simplicity bias: Training a diverse set of models discovers solutions with superior ood generalization. In *Proceedings of the IEEE/CVF conference on computer vision and pattern recognition*, pages 16761–16772, 2022.

Guillermo Valle-Perez, Chico Q Camargo, and Ard A Louis. Deep learning generalizes because the parameter-function map is biased towards simple functions. *arXiv preprint arXiv:1805.08522*, 2018.

Huaxiu Yao, Yu Wang, Sai Li, Linjun Zhang, Weixin Liang, James Zou, and Chelsea Finn. Improving out-of-distribution robustness via selective augmentation. In *International Conference on Machine Learning*, pages 25407–25437. PMLR, 2022.

Haotian Ye, James Zou, and Linjun Zhang. Freeze then train: Towards provable representation learning under spurious correlations and feature noise. In *International Conference on Artificial Intelligence and Statistics*, pages 8968–8990. PMLR, 2023.

Jingzhao Zhang, Aditya Menon, Andreas Veit, Srinadh Bhojanapalli, Sanjiv Kumar, and Suvrit Sra. Coping with label shift via distributionally robust optimisation. *arXiv preprint arXiv:2010.12230*, 2020.

Michael Zhang, Nimit S Sohoni, Hongyang R Zhang, Chelsea Finn, and Christopher Ré. Correct-n-contrast: A contrastive approach for improving robustness to spurious correlations. *arXiv preprint arXiv:2203.01517*, 2022.

A Additional Experiments on MLP

To ensure consistency of results across different architectures, we repeated all experiments, except for those in Subsection 3.3, using a multi-layer perceptron (MLP). The MLP has 10 hidden layers, each containing a linear layer with a width of 1024, followed by batch normalization and ReLU activation. The final layer is linear. Other training setups are the same as those in Section 3. From the results below, we observe the hierarchical decision-making process in MLP, although it is not as pronounced as in the ResNet architecture for the corrupted CIFAR-10 dataset.

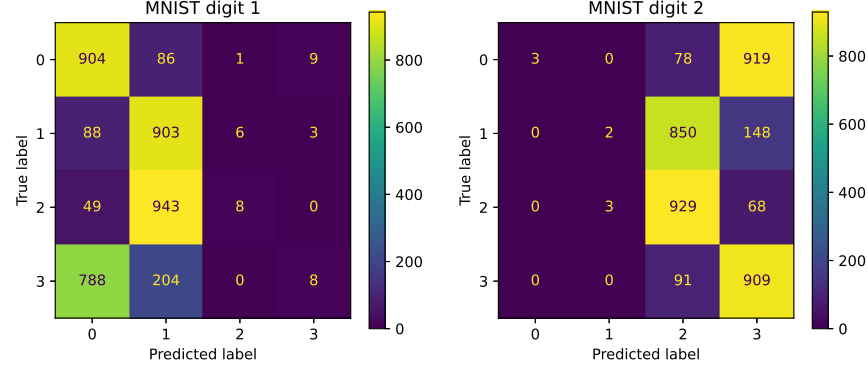


Figure 11: The confusion matrices for the MLP trained on the MNIST-CIFAR dataset.

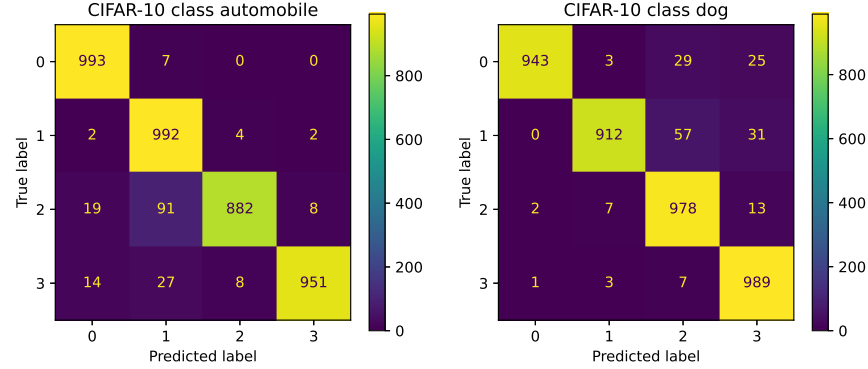


Figure 12: The confusion matrices for the MLP trained on the CIFAR-MNIST dataset.

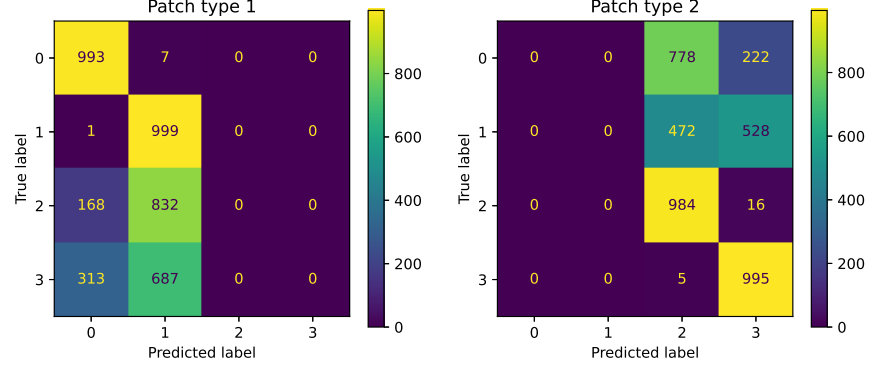


Figure 13: The confusion matrices for the MLP trained on the Patch-MNIST dataset.

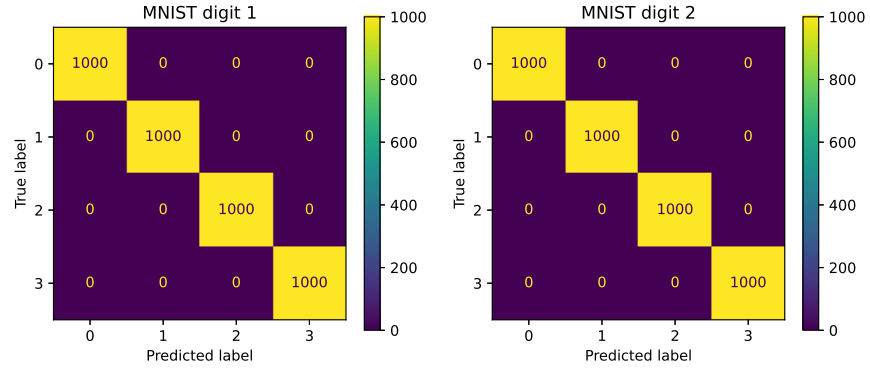


Figure 14: The confusion matrices for the MLP trained on the MNIST-Patch dataset.

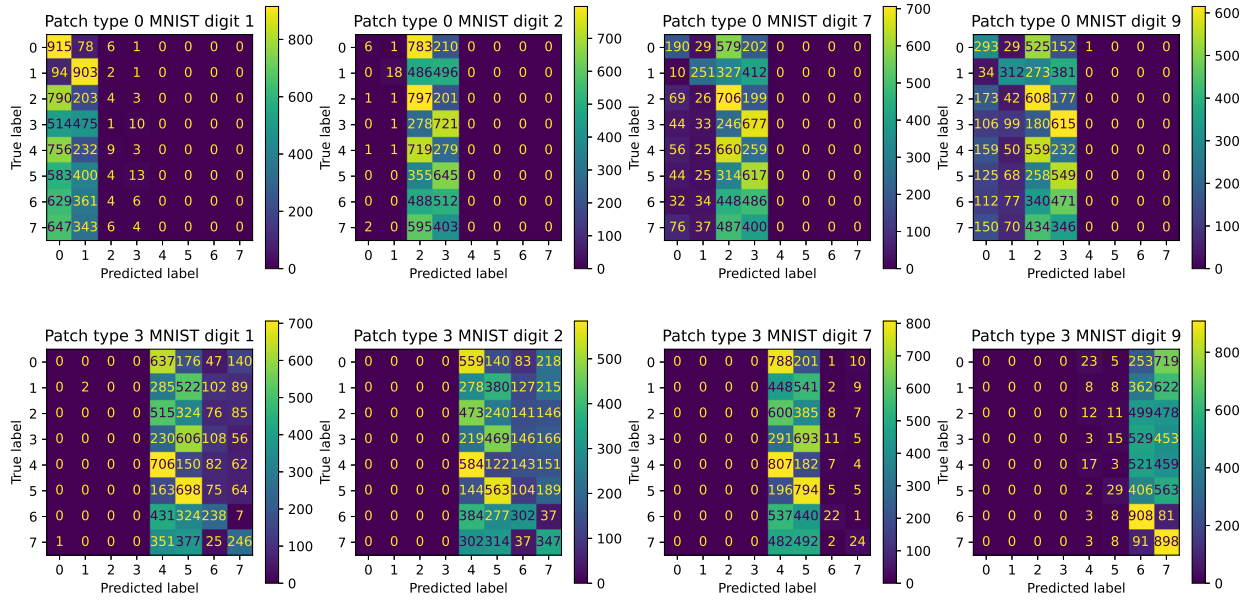


Figure 15: The confusion matrices for the MLP trained on the Patch-MNIST-CIFAR dataset.

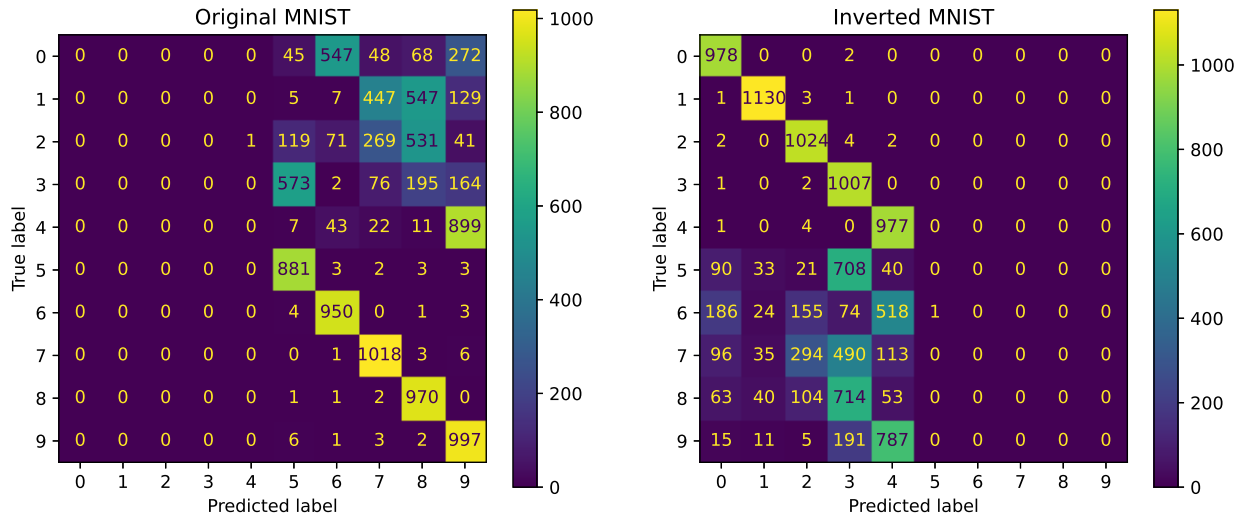


Figure 16: The confusion matrices for the MLP trained on the half-inverted MNIST dataset.

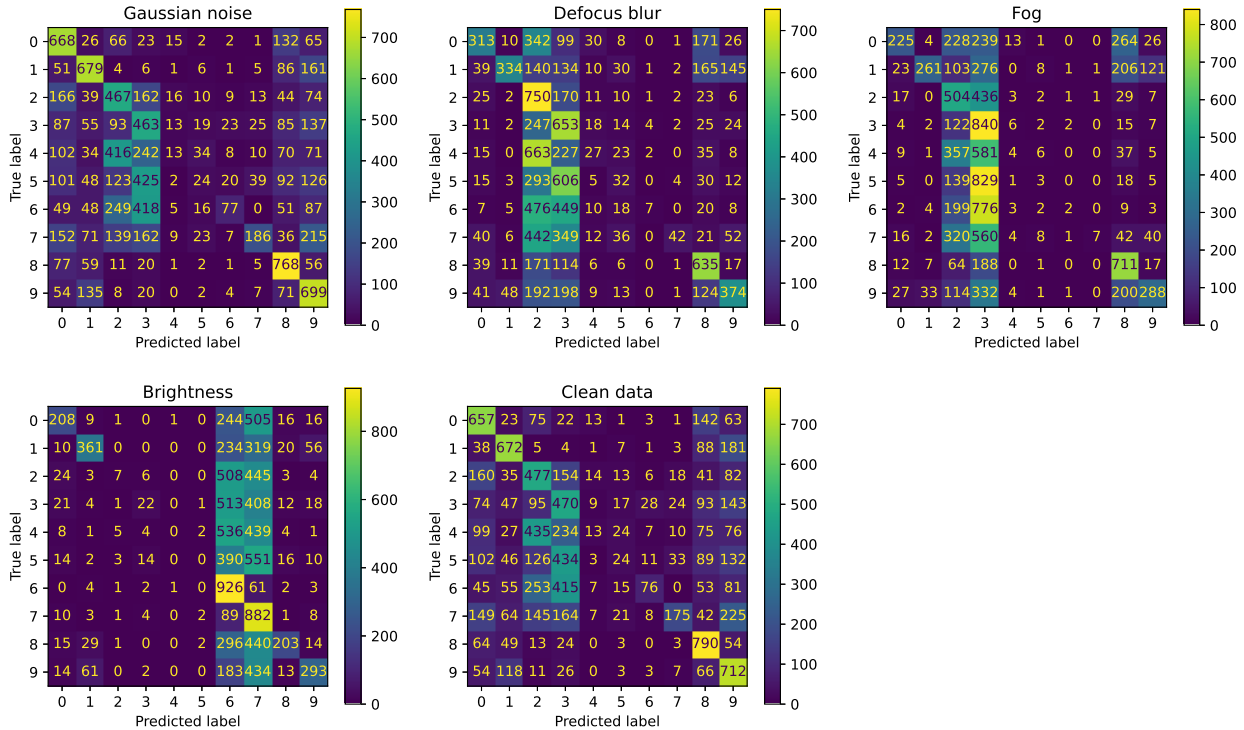


Figure 17: The confusion matrices for the MLP trained on the corrupted CIFAR-10 dataset.